Materials Physics and Mechanics 44 (2020) 238-249 Received: May 25, 2019

VIBRATION OF A HYDROSTATIC STRESSED PIEZOELECTRIC LAYER EMBEDDED ON GRAVITATING HALF SPACE WITH SLIDING INTERFACE BOUNDARY

Rajendran Selvamani*

Department of Mathematics, Karunya Institute of Technology and Sciences,

Coimbatore-641 114, Tamil Nadu, India

*e-mail: selvam1729@gmail.com

Abstract. In this paper, an analytical model is developed to study the influence of initial hydrostatic stress and piezo elasticity on elastic waves in a piezoelectric layer embedded on a gravitating half space with slip interface. The piezo electric layer considered for this study is hexagonal (6mm) material. The problem is described using equations of linear elasticity with initial hydrostatic stress and piezo elastic inclusions. Displacement functions in terms of velocity potential are introduced to separate the motion's equations and electric conduction equations. The frequency equations are obtained by stress free and electrically shorted boundary conditions at the gravitating half space. The numerical computation is carried out for the PZT-4A material. The obtained results are presented graphically to show the effect of piezo elastic coupling and hydrostatic stress on the elastic waves.
Keywords: elastic waves, piezoelectric layers, hydrostatic stress, slip interface, NEMS

1. Introduction

The composite medium consisting of piezo elastic layer and gravitating half space is the important topic in the seismology and construction field due to the self-monitoring and controlling ability of the coupled system. The study of elastic waves in smart materials like piezo electric is utilized in the pattern recognition field, sensing, and activation process with electro-mechanical energy transition and high frequencies-small wavelengths characteristics. The elastic waves of compression type in a circular cylinder made of hexagonal symmetry and anisotropy property were initially developed under the linear theory of elasticity Morse [1]. Bhimaraddi[2] developed a higher order theory for the free vibration analysis of a circular cylindrical shell. Zhang [3] investigated the parametric analysis of the frequency of rotating laminated composite cylindrical shell using wave propagation approach.

Piezoelastic components generated by piezo electric field contribute a mechanism to sense the chaotic nature of mechanical signal coming from perturbed electric potential, to alter the response of the structure by the force given by electric fields. The wave propagation in acoustic meta materials with resonantly shunted cross-shape piezos was studied elaborately by Chen [4]. Thorp et al. [5] investigated the attenuation and localization of wave propagation in rods with periodic shunted piezoelectric patches. The effect of initial stress on the lateral modes in 1-3 piezocomposites is reads from Zhang et al. [6]. Later, Zhang et al. [7] studied the effects of surface piezoelectricity and nonlocal scale on wave propagation in piezoelectric nanoplates. The behavior of Love-type waves in polarized ceramics, piezoelectric half-space carrying FGM layer, has been investigated by Qian et al. [8]. Jin et al. [9] investigated the transmission behavior of Love type surface waves in

http://dx.doi.org/10.18720/MPM.4422020_8

piezoelectric medium under the effect of homogeneous and inhomogeneous initial stress. Recently, the analytic model for Rayleigh wave propagation in piezoelectric layer overlaid orthotropic substratum has been given by Chaudhary et al. [10]. An analytical solution is achieved by Peyman Yaz- danpanah Moghadam et al. [11] for a piezolaminated rectangular plate with arbitrary clamped and simply supported boundary conditions under thermo-electro-mechanical loadings. Sabzikar Boroujerdy and Eslami[12] studied the axisymmetric snap-through nature of Piezo-FGM shallow clamped spherical shells under thermo-electro-mechanical loading. They found that the coupling effect of piezo elasticity enhances the elastic behavior of the FGM shell.

Further, Selvamani and Ponnusamy investigated the elasto dynamic wave propagation in a transversely isotropic piezoelectric circular plate immersed in fluid [13]. Dynamic response of a heat conducting solid bar of polygonal cross sections subjected to moving heat source was studied by [14]. Selvamani [15] investigated the free vibration analysis of rotating piezoelectric bar of circular cross section immersed in fluid. Influence of thermo-piezoelectric field in a circular bar subjected to thermal loading due to laser pulse is reads from Selvamani [16]. Selvamani [17] analyzed the effect of non-homogeneity in a magneto electro elastic plate of polygonal cross-sections. The presence of initial hydrostatic stress in a vibrating medium will produce changes in the elastic properties and material will exhibits anisotropy characteristics. Yu and Tang [18] discussed the dilatational and rotational waves in a magnetoelastic initially stressed conducting medium. De and Sengupta[19] investigated magnetoelastic waves in initially stressed isotropic media. The propagation of elastic waves in an initially stressed magnetoelastic and thermoelastic medium was investigated thoroughly by Acharya and Sengupta [20,21]. The propagation of waves under the influence of gravitating half space is a significant problem in Seismology and Geophysics, which has gained the attention of many researchers Gubbins [22]. Love wave propagation in a fiber-reinforced medium sandwiched between an isotropic layer and gravitating half-space have analyzed by Kundu et al. [23]. Vinh and Anh [24] studied the Rayleigh waves in an orthotropic half-space coated by a thin orthotropic layer with sliding contact.

In the present contribution, vibration in a anisotropic and hydrostatic stressed thermo piezo electric layer resting on gravitating half space is analyzed under linear theory elastic equations. Three displacement equations are considered with its potential derivatives. The frequency equations are obtained for longitudinal and flexural modes at the gravitating half space with stress free and electrically shorted boundary conditions. The numerical results are analyzed for PZT-4 material and the computed stress, displacement, and phase velocity are presented in the form of dispersion curves.

2. Analytical model

A Rectangular Cartesian coordinates are used to study the deformation of piezo electric infinite layer of thickness h. The motion takes place in XZ plane with the origin is considered to be the mid plane of the layer and the Z axis is at right angle to the to the mid plane. The complete governing equations that explain the behavior of piezoelectric layer have been considered from Mindlin [25].

$$\begin{aligned}
\Pi_{xx} &= c_{11}\frac{\partial u}{\partial x} + \left(c_{13} - H_s\right)\frac{\partial w}{\partial z} + e_{31}\frac{\partial \phi}{\partial z},\\
\Pi_{yy} &= c_{12}\frac{\partial u}{\partial x} + \left(c_{13} - H_s\right)\frac{\partial w}{\partial z} + e_{31}\frac{\partial \phi}{\partial z}\\
\Pi_{zz} &= c_{13}\frac{\partial u}{\partial x} + \left(c_{33} - H_s\right)\frac{\partial w}{\partial z} + e_{33}\frac{\partial \phi}{\partial z},\\
\Pi_{xz} &= c_{44}\left(\frac{\partial w}{\partial x} + \frac{\partial u}{\partial z}\right) + e_{15}\frac{\partial \phi}{\partial x}, \Pi_{xy} = 0,\ \Pi_{yz} = 0,
\end{aligned} \tag{1}$$

$$D_x = e_{15}\left(\frac{\partial w}{\partial x}+\frac{\partial u}{\partial z}\right) - \in_{11}\frac{\partial \phi}{\partial x}, D_y = 0,$$

$$D_z = e_{31}\frac{\partial u}{\partial x} + e_{33}\frac{\partial w}{\partial z} - \in_{33}\frac{\partial \phi}{\partial z},$$

where $\Pi_{xx},\Pi_{yy},\Pi_{zz},\Pi_{xy},\Pi_{yz},\Pi_{xz}$ are the stress components, u,w are the displacement components, $c_{11},c_{12},c_{13},c_{33}$ are the elastic constants, e_{31},e_{33} are the piezoelectric constants, $\in_{11},\in_{33}$ represents constants of dielectric, H_s is the initial hydrostatic stress (when $H_s<0$ is hydrostatic tension and $H_s>0$ represents hydrostatic compression), ϕ is the electric potential and ρ_1 is the mass density. The equations of motion for hexagonal (6mm) class are derived as follows

$$c_{11}\frac{\partial^2 u}{\partial x^2} + (c_{13}+c_{44}-H_s)\frac{\partial^2 w}{\partial x \partial z} + c_{44}\frac{\partial^2 u}{\partial z^2} + (e_{31}+e_{15})\frac{\partial^2 \phi}{\partial x \partial z} + \left(e_{31}+e_{15}\right)\frac{\partial^2 u}{\partial x \partial z} = \rho_1\frac{\partial^2 u}{\partial t^2},$$

$$c_{44}\frac{\partial^2 w}{\partial x^2} + \left(c_{33}-H_s\right)\frac{\partial^2 w}{\partial z^2} + (c_{13}+c_{44})\frac{\partial^2 u}{\partial x \partial z} + e_{15}\frac{\partial^2 \phi}{\partial x^2} + e_{33}\frac{\partial^2 \phi}{\partial z^2} = \rho_1\frac{\partial^2 w}{\partial t^2}, \tag{2}$$

$$e_{15}\frac{\partial^2 w}{\partial x^2} + (e_{15}+e_{31})\frac{\partial^2 u}{\partial x \partial z} - \in_{11}\frac{\partial^2 \phi}{\partial x^2} + e_{33}\frac{\partial^2 w}{\partial z^2} - \in_{33}\frac{\partial^2 \phi}{\partial z^2} = 0.$$

3. Solutions of the Field Equation

To obtain the propagation of harmonic waves, the solutions of the displacement vectors in terms of potentials are reads from Paul [26]. Thus, we seek the solution of the Eq. (2) in the following form

$$u = U(z)\sin kx\, e^{i\omega t},$$

$$w = W(z)\cos kx\ e^{i\omega t}, \tag{3}$$

$$\varphi = \left(c_{44}/e_{33}\right)\varphi(z)\cos kx\ e^{i\omega t},$$

where $i=\sqrt{-1}$, k is the wave number, ω is the angular frequency, $U(z),W(z),\phi(z)$ are the displacement potentials. By introducing the following parameters in non dimensional form $x = rh$, $\eta = kh$, $\bar{c}_{ij} = \frac{c_{ij}}{c_{44}}$; $\bar{\varepsilon}_{ij} = \frac{\varepsilon_{11}}{e_{33}}$; $\bar{p} = \frac{p_1 c_{44}}{\beta_3 e_{33}}$, $k_\beta{}^{-2} = \frac{\varepsilon_{ij} c_{44}}{\varepsilon_{33}{}^2}$, $\overline{L_1} = \frac{H_s}{c_{44}}$ and using Eq.(3) in Eq.(2), the following differential equation will be obtained

$$\frac{d^2U}{dr^2} - \eta^2 c_{11}U - (1+\bar{c}_{13}+\overline{L_1})\eta\frac{dW}{dr} - (\bar{e}_{31}+\bar{e}_{15})\eta\frac{d\varphi}{dr} = -(ch)^2 U,$$

$$(1+\bar{c}_{13})\eta\frac{dU}{dr} + (\bar{c}_{33}-\overline{L_1})\frac{d^2W}{dr^2} - \eta^2(W+\varphi) + \frac{d^2\varphi}{dr^2} = -(ch)^2 W, \tag{4}$$

$$(\bar{e}_{31}+\bar{e}_{15})\eta\frac{dU}{dr} - \eta^2\bar{e}_{31}W + \frac{d^2W}{dr^2} - k_{33}{}^{-2}\frac{d^2\varphi}{dr^2} + k_{13}{}^{-2}\eta^2\varphi = 0.$$

The Eq.(4) can be written in the vanishing determinant form as

$$\begin{vmatrix} \frac{d^2}{dr^2}+[(ch)^2-\varepsilon^2 c_{11}] & -(1+\bar{c}_{13})\varepsilon\frac{d}{dr} & (\bar{e}_{31}+\bar{e}_{15})\varepsilon\frac{du}{dr} \\ (1+\bar{c}_{13})\varepsilon\frac{d}{dr} & \bar{c}_{33}\frac{d^2}{dr^2}[(ch)^2-\varepsilon^2] & \frac{d^2}{dr^2}-\bar{e}_{15}\varepsilon^2 \\ [\bar{e}_{31}+\bar{e}_{15}]\varepsilon\frac{d}{dr} & \frac{d^2}{dr^2}-\bar{e}_{15}\varepsilon^2 & k_{33}{}^{-2}\left(\bar{e}_{11}\varepsilon^2-\frac{d^2}{dr^2}\right) \end{vmatrix}\left(U,W,\varphi\right)=0. \tag{5}$$

Evaluating the determinant given in Eq.(5), we obtain a differential equation of the form

$$\left(\frac{d^8}{dr^8}+M\frac{d^6}{dr^6}+N\frac{d^4}{dr^4}+O\frac{d^2}{dr^2}+P\right)(U,W,\varphi)=0, \tag{6}$$

where the constant coefficient M,N,O and P is obtained as follows

$$\begin{aligned}
M &= g_9(g_7\bar{c}_{33}+2g_6-g_1g_{10}\bar{c}_{33}-g_1-g_2^2g_{10}-2g_2g_3-g_3^2\bar{c}_{33}-g_9g_5g_{10})+g_8(-g_{10}\bar{c}_{33}-1)\\
&\quad+\bar{p}^2\bar{c}_{33}-g_7g_5g_{10}+2\bar{p}-g_{10}]/[-g_9(g_{10}\bar{c}_{33}+1)]\\
N &= [g_8(g_7\bar{c}_{33}+2g_6-g_1g_{10}\bar{c}_{33}-g_1-g_2^2g_{10}-2g_2g_3-g_3^2\bar{c}_{33})\\
&\quad+g_9(g_5g_7-g_6^2+g_1g_7\bar{c}_{33}-g_1g_{10}g_5+2g_1g_6+g_2^2g_7+2g_2g_6g_3+g_3^2g_5)\\
&\quad+\bar{p}(g_5\bar{p}+g_1\bar{p}\bar{c}_{33}+2g_1-2g_6+g_2^2\bar{p}+2g_2g_4+2g_2g_3-2g_3g_4\bar{c}_{33})g_7\\
&\quad-g_1g_{10}-2g_2g_4g_{10}+g_3^2-2g_3g_4+g_4^2g_{10}\bar{c}_{33}+g_4^2]/[-g_9(g_{10}\bar{c}_{33}+1)]\\
O &= g_8(g_5g_7-g_6^2+g_1g_7\bar{c}_{33}-g_1g_5g_{10}+2g_1g_6+g_2^2g_7+2g_2g_3g_6+g_3^2g_5)\\
&\quad+g_9(g_1g_5g_7-g_1g_6^2+g_1(g_5\bar{p}^2+g_7-2\bar{p}g_6)+g_3(-g_4g_5\bar{p}+2g_4g_6-\bar{p}g_4g_5)\\
&\quad+g_4(-g_2g_6\bar{p}+2g_1g_6+2g_2g_7-\bar{p}g_2g_6-g_4g_5g_{10}-2g_4g_6)]/[-g_9(g_{10}\bar{c}_{33}+1)],\\
P &= (g_1g_8-g_4^2)(g_5g_7-g_6^2)/[-g_9(g_{10}\bar{c}_{33}+1)]
\end{aligned} \tag{7}$$

with

$$\begin{aligned}
&g_1=(ch)^2-\varepsilon^2\bar{c}_{11}\quad g_2=(1+\bar{c}_{13})\varepsilon\quad g_3=(\bar{e}_{31}+\bar{e}_{15})\varepsilon\quad g_4=\beta\varepsilon^2\quad g_5=(ch)^2-\varepsilon^2\\
&g_6=\varepsilon^2\bar{e}_{11}\quad g_7=\varepsilon^2\bar{e}_{11}/k^2_{33}\quad g_8=\left(\rho c_u c_{44,}/\beta^2{}_3T_0-ik_1\varepsilon^2\right)\quad g_9=ik_3\quad g_{10}=1/k^2_{33}.
\end{aligned} \tag{8}$$

Upon solving the Eq.(6) for the mode in symmetric form is as follows

$$\begin{aligned}
U&=\sum_{i=1}^{4}A_i\cosh(\alpha_i r),\\
W&=\sum_{i=1}^{4}A_i a_i\sinh(\alpha_i r),\\
\varphi&=\sum_{i=1}^{4}A_i b_i\cosh(\alpha_i r),
\end{aligned} \tag{9}$$

and the solutions for an anti-symmetric mode are obtained as by changing the $\cosh(\alpha_i r)$ in to $\sinh(\alpha_i r)$ and vice versa. Here, A_i is the arbitrary constant which is to be determined and $\alpha_i^2>0,(i=1,2,3,4)$ are the roots of the following algebraic equation

$$\alpha^8+M\alpha^6+N\alpha^4+O\alpha^2+P=0. \tag{10}$$

The value of the constants a_i,b_i and c_i represented in the Eq.(9) is derived from the following relations

$$\begin{aligned}
&(1+\bar{c}_{13})\varepsilon\alpha_i a_i-(\bar{e}_{31}+\bar{e}_{15})\varepsilon\alpha_i b_i+\{\alpha_i^2[(ch)^2-\varepsilon^2\bar{c}_{11})]\}=0,\\
&\bar{c}_{33}\alpha_i^2+[(ch)^2-\varepsilon^2]\}a_i+(\alpha_i^2-\bar{e}_{15}\varepsilon^2)b_i-\varepsilon\alpha_i c_i(1+\bar{c}_{13})\varepsilon\alpha_i=0,\\
&(\alpha_i^2-\bar{e}_{11}\varepsilon^2)a_i+[\varepsilon^2\bar{e}_{11}-\alpha_i^2)]b_i+\varepsilon\bar{p}\alpha_i c_i+(\bar{e}_{31}+\bar{e}_{15})\varepsilon\alpha_i=0.
\end{aligned} \tag{11}$$

4. Formulation of the gravitating half space

The equation of motion of the gravitating half space is reads from Kundu et al. [23]

$$\begin{aligned}
&\coprod_{xx,x}+\coprod_{xz,z}-\rho_2 g w_{,z}=\rho_2 u_{,tt},\\
&\coprod_{xz,z}+\coprod_{zz,z}-\rho_2 g u_{,z}=\rho_2 w_{,tt},
\end{aligned} \tag{12}$$

where g is the acceleration due to gravity $\coprod_{xz}, \coprod_{xx}$ and $\coprod_{zz}$ are the stress components of the half space, the relation between stress and strain for isotropic material is explained as

$$\coprod_{xz} = 2\mu e_{xz},$$

$$\coprod_{zz} = (\lambda + 2\mu)e_{zz} + \lambda e_{xx}, \tag{13}$$

where λ and μ are the Lame's constants and $e_{xx} = \frac{\partial u}{\partial x}$, $e_{zz} = \frac{\partial w}{\partial z}$ and $e_{xz} = \frac{1}{2}\left(\frac{\partial u}{\partial z} + \frac{\partial w}{\partial x}\right)$. Using equation (13) in (1) we obtain the following relations with displacement components

$$\mu\left(\frac{\partial^2 u_1}{\partial z^2} + \frac{\partial^2 w_1}{\partial x \partial z} + 2\frac{\partial^2 u_1}{\partial x^2}\right) + \lambda\left(\frac{\partial^2 w_1}{\partial x \partial z} + \frac{\partial^2 u_1}{\partial x^2}\right) - \rho_2 g \frac{\partial w_1}{\partial x} = \rho_2 \frac{\partial^2 u_1}{\partial t^2},$$

$$\mu\left(2\frac{\partial^2 w_1}{\partial z^2} + \frac{\partial^2 u_1}{\partial x \partial z} + 2\frac{\partial^2 w_1}{\partial x^2}\right) + \lambda\left(\frac{\partial^2 w_1}{\partial z^2} + \frac{\partial^2 u_1}{\partial x \partial z}\right) + \rho_2 g \frac{\partial u_1}{\partial x} = \rho_2 \frac{\partial^2 w_1}{\partial t^2}, \tag{14}$$

we can consider the solution of equation (14) as follows:

$$u_1 = U_1(z)\sin k_1 x\, e^{ip_1 t}, \qquad w_1 = W_1(z)\cos k_1 x\, e^{ip_1 t}, \tag{15}$$

where k_1 is the wave number and p_1 is the circular frequency of the half space. Introducing non dimensional quantity $y = rh,\ \eta_1 = k_1 h$ and substituting the solution in equation(15) in (14) we get

$$\mu\left[\frac{d^2 U_1}{dr^2} - \eta_1 \frac{dW_1}{dr} - 2\eta_1^2 U_1\right] - \lambda\left[\eta_1 \frac{dW_1}{dr} + \eta_1^2 U_1\right] + \rho_2 g \eta_1 h W_1 = -\rho_2 (p_1 h)^2 U_1,$$

$$\mu\left[2\frac{d^2 W_1}{dr^2} + \eta_1 \frac{dU_1}{dr} - 2\eta_1^2 W_1\right] + \lambda\left[\frac{d^2 W_1}{dr^2} + \eta_1 \frac{dU_1}{dr}\right] + \rho_2 g \eta_1 h U_1 = -\rho_2 (p_1 h)^2 W_1. \tag{16}$$

The non-trivial solution of the above differential equation (16) is obtained as follows

$$\begin{vmatrix} \mu\frac{d^2}{dr^2} - 2\mu\eta_1^2 - \lambda\eta_1^2 + \rho_2 (p_1 h)^2 & -(\mu+\lambda)\eta_1 \frac{d}{dr} + \rho_2 g \eta_1 h \\ (\mu+\lambda)\eta_1 \frac{d}{dr} + \rho_2 g \eta_1 h & (2\mu+\lambda)\frac{d^2}{dr^2} - 2\mu\eta_1^2 + \rho_2 (p_1 h)^2 \end{vmatrix} (U_1, W_1) = 0. \tag{17}$$

Taking $e_1 = \mu,\ e_2 = -\mu\eta_1^2,\ e_3 = \lambda\eta_1^2,\ e_4 = \rho_2 (p_1 h)^2,\ e_5 = (\mu+\lambda)\eta_1,\ e_6 = \rho_2 g \eta_1 h,\ e_7 = (2\mu+\lambda)$ and expanding the above determinant, we get

$$\left(\frac{d^4}{dr^4} + R\frac{d^2}{dr^2} + S\right)(U_1, W_1) = 0, \tag{18}$$

where $R = \left(e_1 e_2 + e_1 e_4 + e_2 e_7 + e_3 e_7 + e_4 e_7 + e_5^2\right)/e_1 e_7,\ S = \left(e_2^2 + 2e_2 e_4 + e_2 e_3 + e_3 e_4 + e_4 e_7 + e_5^2\right)/e_1 e_7$. The solutions of the above equation (18) in symmetric and antisymmetric mode are obtained as follows

$$U_1 = \sum_{i=1}^{2} B_i \cosh(\beta_i r),$$

$$W_1 = \sum_{i=1}^{2} B_i q_i \sinh(\beta_i r),$$

$$U_1 = \sum_{i=1}^{2} B_i \sinh(\beta_i r),$$

$$W_1 = \sum_{i=1}^{2} B_i q_i \cosh(\beta_i r). \tag{19}$$

Here, B_i is the arbitrary constant which are to be determined and $\beta_i^2 > 0, (i = 1,2,3,4)$ are the roots of the following algebraic equation

$$\beta^4 + R\beta^2 + S = 0 \tag{20}$$

and the constant q_i is given by the following relation for the isotropic half space

$$-(\mu+\lambda)\eta\beta_i q_i+\rho_2 g\eta h q_i+\mu\beta_i^2+(\rho_2(ph)^2-2\eta^2\mu-\lambda\eta^2)=0,$$
$$(2\mu+\lambda)\beta_i^2 q_i+(\rho_2(ph)^2-2\eta^2)q_i+(\mu+\lambda)\eta\beta_i+\rho_2 g\eta h=0. \quad (21)$$

5. Boundary conditions and Frequency equations

Boundary conditions are constructed for the anisotropic layer and gravitating half space at the interface. Since the layer and the gravitating half space are in sliding contact, then the stress and displacement will becomes

$$\amalg_{xz}=\Pi_{xz}=0,$$
$$\amalg_{zz}=\Pi_{zz}=0, \quad (22)$$
$$U=W_1=0.$$

The thermally insulated and electrically shorted boundary conditions are as follows

$$\varphi=0. \quad (23)$$

Substituting the solutions given in the Eqs. (9) and (17) in the boundary above conditions will lead to a system of algebraic equation for the unknowns $A_{1,}A_{2,}A_3,A_4$ and $B_{1,}B_2$, this system of algebraic equations can be written in the following matrix vector form

$$[A]\{X\}=\{0\}, \quad (24)$$

where $[A]$ is a 6×6 matrix of unknown wave amplitudes, and $\{X\}$ is an 6×1 column vector of the unknown amplitude coefficients. The solution of Eq. (24) is given by the following determinant

$$|A|=[\chi_{ij}],\ i,j=1,2,3,4,5,6,8\ ,$$

in which

$$\chi_{1j}=(c_{13}-c_{14})k+(c_{33}a_j-H_s a_j+c_{44}b_j)\frac{\alpha_j}{h},$$

$$\chi_{2j}=(c_{13}-c_{14})k+(c_{33}a_j-H_s a_j+c_{44}b_j)\frac{\alpha_j}{h},$$

$$\chi_{3j}=c_{44}\frac{\alpha_j}{h}-\left[a_j+e_{15}\left(\frac{c_{44}}{e_{33}}\right)b_j\right]k,$$

$$\chi_{4j}=c_{44}\frac{\alpha_j}{h}-\left[a_j+e_{15}\left(\frac{c_{44}}{e_{33}}\right)b_j\right]k,\ j=1,2,3,4,5,6,\ \chi_{47}=0,\ \chi_{48}=0,$$

$$\chi_{5j}=\mu\left[\frac{a_j}{h}-a_jk\right],\ \chi_{58}=0,\ \chi_{6j}=\left[(\lambda+2\mu)a_j\frac{\alpha_j}{h}+\lambda k\right],$$

$$\chi_{67}=0,\ \chi_{68}=0\ \chi_{7j}=(s_j-\varepsilon^2 q_j\overline{e_{15}}e_j),\ \chi_{78}=0,\ \chi_{8j}=(e_j)g(s_j),$$

$$\chi_{88}=(r_j)f(s_j),\ \chi_{37}=0,\ \chi_{38}=0,$$

$$\chi_{18}=0,\ \chi_{27}=0,\ \chi_{28}=0,\ \chi_{17}=0.$$

6. Numerical results and discussion

To study the effect of hydrostatic stress and applied forces on frequency, we have computed stress, strain, and displacements numerically. For this purpose, we got the values of the relevant material parameters Paul [26]

$c_{11}=13.9\times10^{10}\,Nm^{-2}$, $c_{12}=7.78\times10^{10}\,Nm^{-2}$, $c_{13}=7.43\times10^{10}\,Nm^{-2}$, $c_{33}=11.5\times10^{10}\,Nm^{-2}$, $c_v=420Jkg^{-1}K^{-1}$, $e_{31}=-5.2Cm^{-2}$, $e_{33}=15.1Cm^{-2}$, $e_{15}=12.7Cm^{-2}$, $\in_{11}=6.46\times10^{-9}C^2N^{-1}m^{-2}$, $\in_{33}=5.62\times10^{-9}C^2N^{-1}m^{-2}$, $\rho_1=7500Kgm^{-2}$ and for the gravitating half-space Kundu et al. [20] $\lambda=67.7\,GPa$, $\mu=74.3\,GPa$ and $\rho_2=3.323\ g/cm^3$.

The dispersion curves are drawn in Figs. 1 and 2 for variation of normal stress Π_{xx} versus the wave number of the piezo electric layer for the hydrostatic values with respect to different piezo electric constants. Figure 1 shows the magnitude variation of normal stress modes when wave number is increasing for the different values of hydrostatic stress. Figure 2 reveals the oscillating trend in the wave propagation due to the increase in dielectric constant values. It can be noted that the effect of hydrostatic pressure and piezoelectric constants shows an increasing effect on the stress magnitude. A comparative illustration is made between the normal strain and the wave number s of the layer for the piezo electric constant values of vibration is respectively shown in Figs. 3 and 4. From Figs. 3 and 4, it is clear that, the lower range of wave number the normal strain attain minimum value in both cases of piezo electric constants, after that, it starts increases with the increase of hydrostatic stress.

The variation of electrical displacement Dz with respect to the wave number of the piezo electric layer for the various hydrostatic stress with respect to different piezo electric constants is presented in Figs. 5 and 6. The amplitude of electrical displacement increases monotonically to attain maximum value in a lower range of wave number and slashes down to became asymptotically linear in the remaining range of the wave number in Figs. 5 and 6 with increasing values of hydrostatic stresses. From Figs. 5 and 6, it is noticed that the electrical displacement profiles exhibits high oscillating nature in the small wave number range since the energy radiation is more sensitive in the surface areas. The cross over points in the vibrational modes may indicate the energy transfer between the layer and the half space.

The 3D curve in Figs. 7-11 clarifies the complete relation between the physical quantities and the distance components in the presence of hydrostatic stress, gravity, and electrical constants. From these obtained results, it is understood that the physical components are highly dependent on the variation of distance from the origin. These studies are also explaining the dependence of dielectric and hydrostatic stress values on physical quantities.

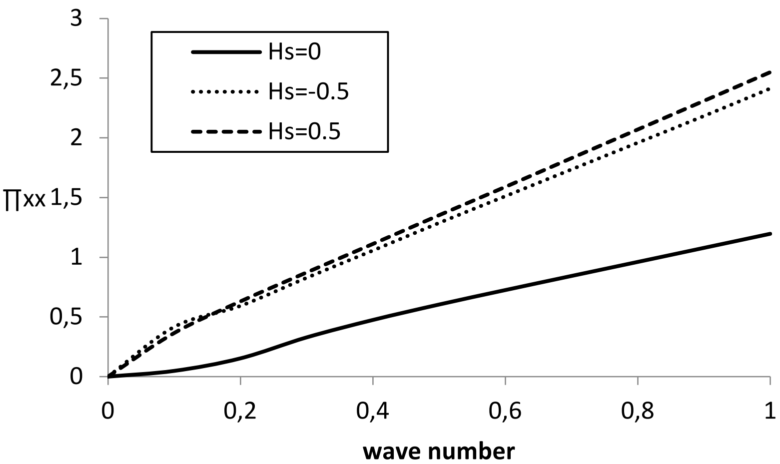

Fig. 1. Variation of radial stress with wave number ($e_{31} = -2.5$, $e_{33} = 5.2$, $e_{15} = 6.5$)

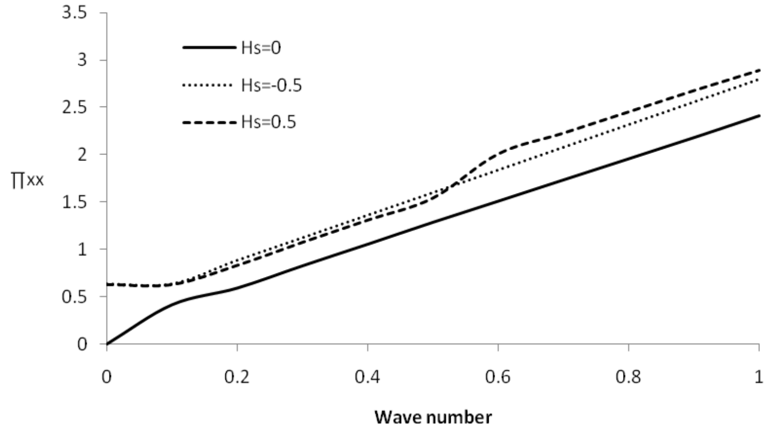

Fig. 2. Variation of radial stress with wave number ($e_{31} = -2.5$, $e_{33} = 10.2$, $e_{15} = 11.5$)

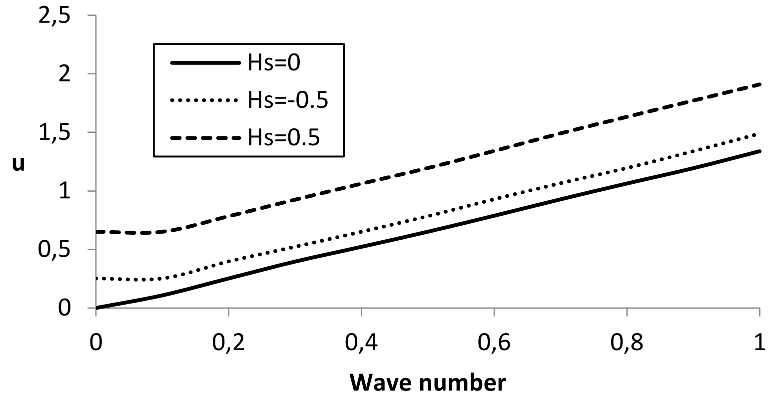

Fig. 3. Variation of displacement with wave number ($e_{31} = -2.5$, $e_{33} = 5.2$, $e_{15} = 6.5$

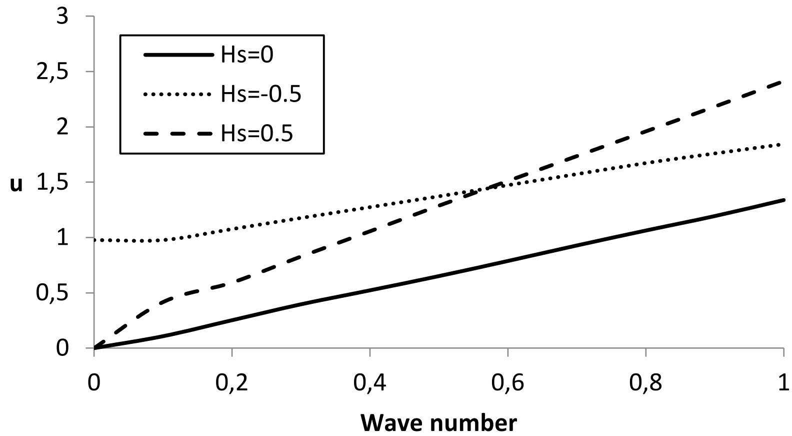

Fig. 4. Variation of displacement with wave number ($e_{31} = -2.5$, $e_{33} = 10.2$, $e_{15} = 11.5$)

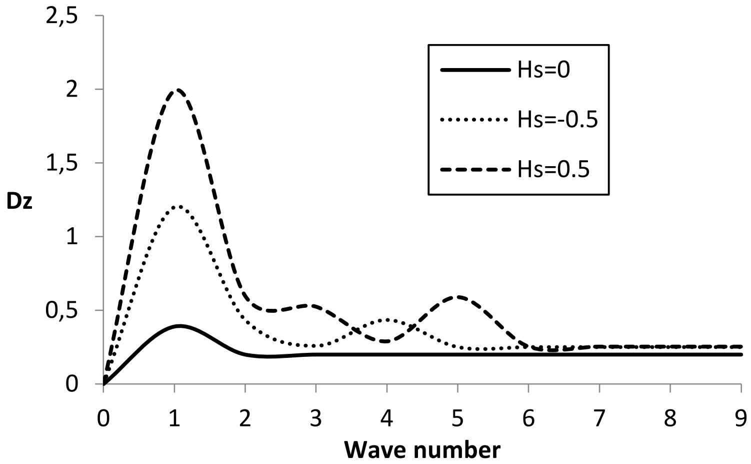

Fig. 5. Variation of displacement with wave number ($e_{31} = -2.5$, $e_{33} = 5.2$, $e_{15} = 6.5$)

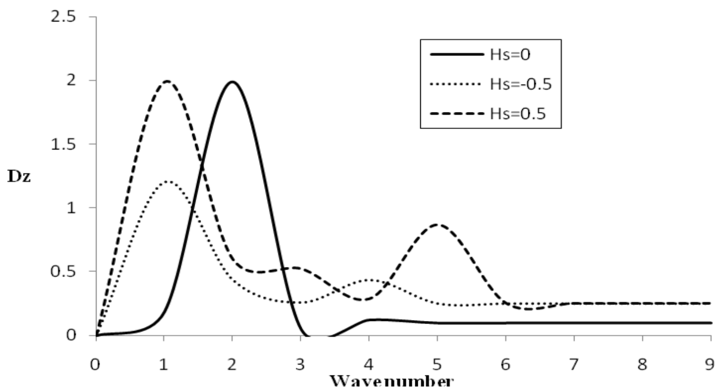

Fig. 6. Variation of displacement with wave number($e_{31} = -2.5$, $e_{33} = 10.2$, $e_{15} = 11.5$)

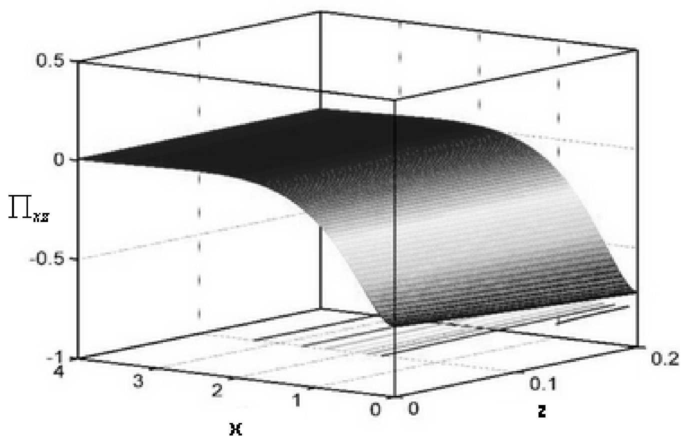

Fig. 7. 3D Distribution of stress with $\in_{11} = 7.36$, $\in_{33} = 6.62$, $Hs = 0.5$ and $g = 0.5$

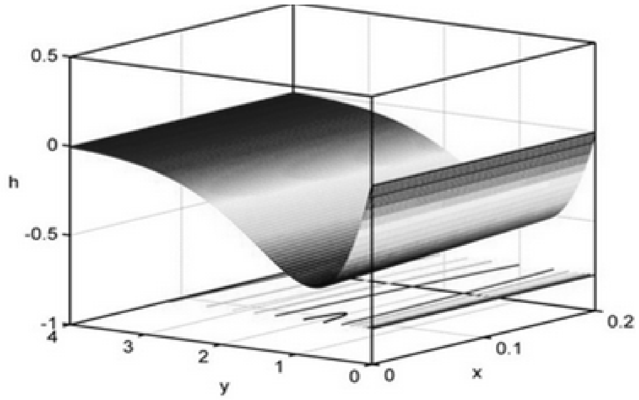

Fig. 8. 3D Distribution of thickness with $\in_{11} = 7.36$, $\in_{33} = 6.62$, $Hs = 0.5$ and $g = 0.5$

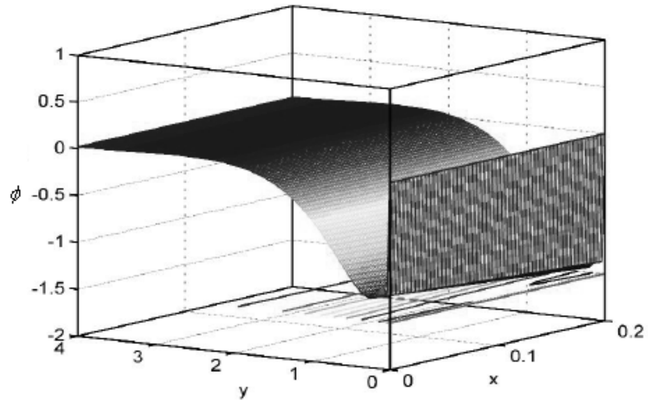

Fig. 9. 3D Distribution of electric potential with $\in_{11} = 7.36$, $\in_{33} = 6.62$, $Hs = 0.5$ and $g = 0.5$

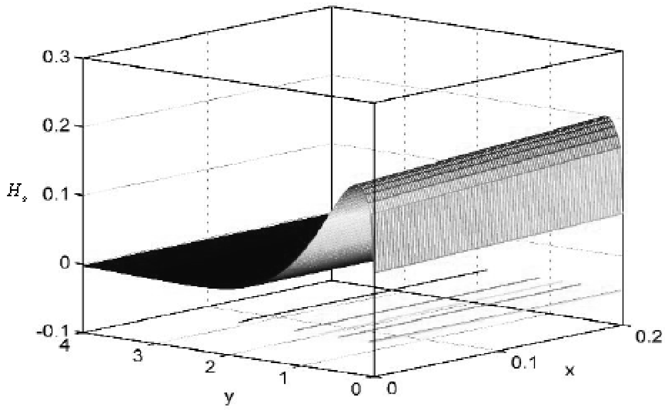

Fig. 10. 3D Distribution of hydro static stress with $\in_{11} = 7.36$, $\in_{33} = 6.62$, $Hs = 0.5$ and $g = 0.5$

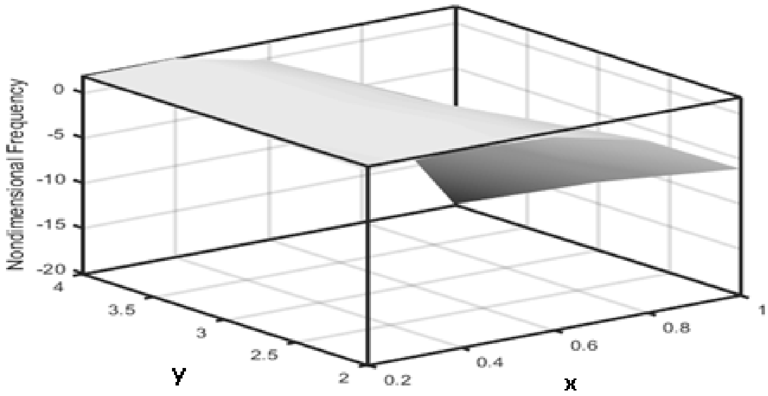

Fig. 11. 3 D Distribution of non-dimensional frequency with $\in_{11} = 7.36$, $\in_{33} = 6.62$, and $g = 0.5$

7. Conclusions

This study demonstrates the effect of hydrostatic stress and piezo electric effect on elastic waves of an elastic layer embedded in a gravitating half space. The equation of motion is derived using two dimensional elastic equations coupled with piezo electric and gravitating half space. The frequency equations are obtained for free stress and insulated electrical boundary conditions at the gravitating half space. The numerical results are analyzed for PZT-4 material and the computed stress, displacement, electrical displacement, and some important physical quantities are presented in the form of dispersion curves. From the results indicated, we can conclude that

1. The hydro static stress, electric field, and gravity of the half space play an important role in the variation of all physical quantities. Also the physical quantities increases or decreases as the hydrostatic stress, electric field and gravity increases.

2. The values of stress and displacements attain maximum amplitude in the lower wave number (Higher wave length) range.

3. The phenomenon of distance dependence of physical quantities is indicated in Figures.

4. This type of results presented here, will provide useful information for researchers in seismic science to understand the seismic response of elastic waves in medium coupled with piezoelectric layer and some field forces. The physical property of gravitating half space and the interacting medium is a very useful theory in the field of geophysics and earthquake engineering and seismologist working in the field of mining tremors and drilling into the earth's crust.

Acknowledgements. *No external funding was received for this study.*

References

[1] Morse RW. Compressional waves along an anisotropic circular cylinder having hexagonal symmetry. *J. Acoust. Soc. America.* 1954;26(6): 1018-1021.

[2] Bhimraddi AA. A higher order theory for free vibration analysis of circular cylindrical shell. *Int. J. Solid and Struct*. 1984;20(7): 623-630.

[3] Zhang XM. The parametric analysis of frequency of rotating laminated composite cylindrical shell using wave propagation approach. *Comp. methods. Appl. Mech. Eng*. 2002;191(19-20): 2027-2043.

[4] Chen S. Wave propagation in acoustic met materials with resonantly shunted cross-shape piezos. *J. Intelligent Mater. Syst. Struct.* 2018;29(3): 2744-2753.

[5] Thorp O, Ruzzene M, Baz A. Attenuation and localization of wave propagation in rods with periodic shunted piezoelectric patches. *Smart Mater. Struct*. 2001;10(5): 979-989.
[6] Zhang H, Shen Y, Li Y, Mei X. Effect of initial stress on the lateral modes in 1-3 piezocomposites. *Mech. Adv. Mater. Struct*. 2013;20(2): 122-129.
[7] Zhang LL, Liu JX, Fang FQ and Nie GQ. Effects of surface piezoelectricity and nonlocal scale on wave propagation in piezoelectric nano plates. *European.J. Mech- A/Solids*. 2014;46: 22-29.
[8] Qian Z, Jin F, Wang Z. Transverse surface waves on a piezoelectric material carrying a functionally graded layer of finite thickness. *Int. J. Eng. Sci*. 2007;45(2-8): 455-466.
[9] Jin F, Qian Z, Wang Z. Propagation behavior of Love waves in a piezoelectric layered structure with inhomogeneous initial stress. *Smart Mater. Struct*. 2005;14(4): 515-523.
[10] Chaudhary S, Sahu S, Singhal A. Analytic model for Rayleigh wave propagation in piezoelectric layer overlaid orthotropic substratum. *Act. Mech*. 2017;228(2): 495-529.
[11] Yazdanpanah Moghadam P, Tahani M, Naserian-Nik AM. Analytical solution of piezolaminated rectangular plates with arbitrary clamped/simply-supported boundary conditions under thermo-electro-mechanical loadings. *Appl.Mathe. Modelling.* 2003;37(5): 3228-3241.
[12] Sabzikar Boroujerdy M, Eslami MR. Axisymmetric snap-through behavior of Piezo-FGM shallow clamped spherical shells under thermo-electro-mechanical loading. *Int. J. Press. Vessels. Piping.* 2014;120-121: 19-26.
[13] Selvamani R, Ponnusamy P. Elasto dynamic wave propagation in a transversely isotropic piezoelectric circular plate immersed in fluid. *Mater. Phys. Mechs*. 2013;17(2): 164-177.
[14] Selvamani R. Dynamic response of a heat conducting solid bar of polygonal cross sections subjected to moving heat source. *Mater. Phys. Mechs*. 2014;21(2): 177-193.
[15] Selvamani R. Free vibration analysis of rotating piezoelectric bar of circular cross section immersed in fluid. *Mater. Phys. Mechs*. 2015;24(1): 24-34.
[16] Selvamani R. Influence of thermo-piezoelectric field in a circular bar subjected to thermal loading due to laser pulse. *Mater. Phys. Mechs*. 2016;27(1): 1-8
[17] Selvamani R. Effect of non-homogeneity in a magneto electro elastic plate of polygonal cross-sections. *Mater. Phys. Mechs*. 2018;40(1): 84-103.
[18] Yu CP, Tang S. Magneto-elastic waves in initially stressed conductors. *Z Angew Math Phys*. 1966;17(6): 766-775.
[19] De SN, Sengupta PR. Magneto-elastic waves and disturbances in initially stressed conducting media. *Pure. Appl. Geophys.* 1972;93: 41-54.
[20] Acharya DP, Sengupta PR. Magneto-thermo-elastic waves in an initially stressed conducting layer. *Gerlands Beitr Geophys.* 1978;87: 229-239.
[21] Acharya DP, Sengupta PR. Magneto-thermo-elastic surface waves in initially stressed conducting media. *Acta. Geophys. Polonica.* 1978;26: 299-311.
[22] Gubbins D. *Seismology and plate tectonics*. Cambridge: Cambridge University Press; 1990.
[23] Kundu S, Pandit DK, Gupta S, Manna S. Love wave propagation in a fiber-reinforced medium sandwiched between isotropic layers and gravitating half-space. *J. Eng. Math*. 2016;100(1): 109-119.
[24] Vinh PC, Anh VTN. Rayleigh waves in an orthotropic half-space coated by a thin orthotropic layer with sliding contact. *Int. J. Eng. Sci*. 2014;75: 154-164.
[25] Mindlin RD. Equation of high frequency vibrations of thermo-piezoelectric crystal plates. In: Parkus H. (ed.) *Electromagnetic Interactions in Elastic Solids Interactions in Elastic Solids*. Wien: Springer; 1979.
[26] Paul HS, Renganathan K. Free vibration of a pyroelectric layer of hexagonal (6mm) class. *J. Acoust.Soc. America.* 1985;78(2): 395-397.